frontiers in Physics

ORIGINAL RESEARCH
published: 07 February 2020
doi: 10.3389/fphy.2019.00250

Entropy Generation in $C_6H_9NAO_7$ Fluid Over an Accelerated Heated Plate

Tarek Nabil Ahmed [1,2]* *and Ilyas Khan* [1,3]*

[1] Basic Engineering Sciences Department, College of Engineering Majmaah University, Al-Majmaah, Saudi Arabia, [2] Mathematics Department, Faculty of Science, Beni-Suef University, Beni-Suef, Egypt, [3] Department of Mathematics, College of Science Al-Zulfi, Majmaah University, Al-Majmaah, Saudi Arabia

This study considers sodium-alginate ($C_6H_9NaO_7$) fluid over an accelerated vertical plate. The plate is heated from the bottom. A non-Newtonian model of $C_6H_9NaO_7$ is considered. The convection term in the momentum equations is also considered. The dimensionless form of the problem is constructed based on dimensionless variables. The integral transformation of Laplace is used to develop the exact solution to the problem. Explicit expressions are obtained for the velocity field and temperature distribution. The corresponding skin-friction and Nusselt number results are computed based on this. Equations for entropy generation (EG) and Bejan number (BN) are developed. The results are plotted and discussed for embedded parameters. Most significantly, the results for EG and BN are computed and discussed.

Keywords: heat transfer, entropy generation, Casson fluid, exact solutions, integral transform

OPEN ACCESS

Edited by:
Sara I. Abdelsalam, National Autonomous University of Mexico, Mexico

Reviewed by:
Kh S. Mekheimer, Al-Azhar University, Egypt
Abdullah Zaher, Benha University, Egypt
Hina Sadaf, National University of Sciences and Technology, Pakistan

***Correspondence:**
Tarek Nabil Ahmed
t.ahmed@mu.edu.sa
Ilyas Khan
i.said@mu.edu.sa

Specialty section:
This article was submitted to Mathematical Physics, a section of the journal Frontiers in Physics

Received: *20 October 2019*
Accepted: *23 December 2019*
Published: *07 February 2020*

Citation:
Ahmed TN and Khan I (2020) Entropy Generation in $C_6H_9NAO_7$ Fluid Over an Accelerated Heated Plate. Front. Phys. 7:250. doi: 10.3389/fphy.2019.00250

INTRODUCTION

Entropy generation (EG) is a tool that helps to assess improved results, enhance achievements, and reduce the loss of energy in thermal engineering systems (TES) [1]. Recently, this technique has been applied to TES operating with nanofluids [2]. The EG method is used to develop performance standards for thermal engineering equipment. In the literature, Bejan is considered to be the first to point out the various factors behind EG [3, 4] in TES. Bejan [5] introduced the EG number, referred to as the Bejan number, which is the ratio of EG due to heat transfer to the total EG of the system. Moreover, he indicated the conditions of the second law of thermodynamics related to the convection problems of nanofluids. Selimefendigil et al. [6] demonstrated the magnetic-resistive convection flow of nanofluids (CuO-water and Al_2O_3-water) in a restricted trapezoidal cavity. Quing et al. [7] investigated EG in radiative flow of Casson nanofluids over permeable stretchable sheets. A detailed review of EG in nanofluid flow was presented by Mahian et al. [8], who collected and critically discussed recent studies with a wide range of applications. The study organized different aspects of heat-transfer problems and EG in the current state of the art, making suggestions for useful future directions.

Darbari et al. used the response surface method (RSM) to conduct a numerical sensitivity analysis of the effect of nanoparticles (Al_2O_3) in water-based nanofluids on EG [9]. The results indicated that the total EG comprised EG due to friction and due to heat conduction. The sensitivity analysis of EG highlighted the influence of the Reynolds number, particle size, and solid-volume fraction. Ellahi et al. [10] mathematically analyzed EG in natural-convection boundary-layer flow of nanofluids near an inverted cone. It was found that EG was produced because of nanoparticles. Sheikholislami et al. [11] revealed that the EG and heat-transfer rate were enhanced by volume friction and Rayleigh number during the flow of various types of nanofluids in a cavity containing

square-shell rectangular heated objects. Saqib et al. [12] developed a Caputo-type fractional model for the mixed-convection flow of different types of nanofluids. The exact analytical results for velocity, temperature, EG, and Bejan number were obtained via the Laplace-transform technique and presented in figures and tables with physical explanations. Khan et al. [13] described the EG in unsteady magnetic fluid dynamics (MHD) flow through porous media, combining the effects of mass and heat transfer. The effects of several factors on EG, Bejan number, and velocity distribution were reported in numerous figures. Bhatti et al. [14] analyzed the EG of Eyeling-Powell nanofluids through a permeable stretchable surface. The effects of magnetohydrodynamics (MHD) and non-linear thermal radiation were also considered. Li et al. [15] considered EG in forced-convection flow of Al_2O_3-water nanofluids. They reported the impact of Reynolds number (Re), height ratio, and pitch ratio on EG.

Khan et al. [16] obtained an exact solution for the problem of convection-MHD flow of sodium-alginate-based Casson-type nanofluids with the effects of MHD and Newtonian heating. Haq et al. [17] used an exact analysis and developed an exact solution for the free-convection problem of viscous fluid, which depends strongly on time and the slippage condition. Khan et al. [18] generated exact solutions for a rotating viscous fluid such that the fluid exhibits eccentric-concentric rotation. Ahmed and Khan [19] examined the mixed-convection flow of SA-NaAlg nanofluids such that the base fluid is taken as MoS_2. Khater et al. [20, 21] studied two different problems using the magnetohydrodynamics effect with a Hall current. In this problem, the analysis of entropy generation is considered for Casson fluid over an accelerated plate. The problem in dimensionless form is solved by using the Laplace transform technique, and the results are plotted and discussed.

DESCRIPTION OF THE PROBLEM

Consider the unsteady, incompressible mixed-convection flow of a Casson fluid near an infinite vertical plate. It is assumed that, at $\tau \leq 0$, the system is at rest at a temperature of θ_∞. At $\tau = 0^+$, the plate starts moving with a variable velocity of $v(0,\tau) = A\tau$, and the temperature of the plate increases from $\theta(\eta,0) = \theta_\infty$ to $\theta(0,\tau) = \theta_w$. At this stage, mixed convection occurs owing to the change in temperature and the motion of the plate. The initial fluid motion is in the vertical direction and is governed by the following partial differential equations (momentum and energy equations) [16, 19].

$$\rho\frac{\partial v(\eta,\tau)}{\partial\tau} = \mu\left(1+\frac{1}{\beta}\right)\frac{\partial^2 v}{\partial\eta^2} + \rho g\beta_\theta\left(\theta(\eta,\tau)-\theta_\infty\right), \quad (1)$$

$$\rho c_p\frac{\partial\theta(\eta,\tau)}{\partial\tau} = k\frac{\partial^2\theta(\eta,\tau)}{\partial\eta^2}, \quad (2)$$

These are associated with the following physical initial and boundary conditions.

$$\left.\begin{array}{l} V(\eta,0)=0,\quad \theta(\eta,0)=\theta_\infty \\ v(0,\tau)=A\tau,\ v(\infty,\tau)=0 \\ \theta(0,\tau)=\theta_w,\ \theta(\infty,\tau)=\theta_\infty \end{array}\right\}, \quad (3)$$

where ρ is the density, $v(\eta,\tau)$ the x-component of the velocity vector, μ the dynamic viscosity, g the gravitational acceleration, β_θ the volumetric thermal expansion, $\theta(\eta,\tau)$ the x-component of the temperature vector, c_p the heat capacitance, and k the thermal conductivity of the fluid. To remove the units, the following dimensionless variables are introduced into Equations (1)–(3).

$$v^* = \frac{v}{(vA)^{\frac{1}{3}}},\ \eta^* = \frac{\eta A^{\frac{1}{3}}}{v^{\frac{2}{3}}},\ \tau^* = \frac{\tau A^{\frac{2}{3}}}{v^{\frac{1}{3}}},\ \theta^*(\eta,\tau) = \frac{\theta-\theta_\infty}{\theta_w-\theta_\infty},$$

This yields the following form.

$$\frac{\partial v}{\partial\tau} = \left(1+\frac{1}{\beta}\right)\frac{\partial^2 v}{\partial\eta^2} + Gr\theta, \quad (4)$$

$$\Pr\frac{\partial\theta}{\partial\tau} = \frac{\partial^2\theta}{\partial\eta^2}, \quad (5)$$

$$\left.\begin{array}{lll} V(\eta,0)=0, & v(0,\tau)=\tau, & v(\infty,\tau)=0 \\ \theta(0,\tau)=1, & \theta(\infty,\tau)=0, & \theta(\eta,0)=0 \end{array}\right\}, \quad (6)$$

where $Gr = \frac{g\beta_\theta\Delta\theta}{A}$,$\Pr = \frac{\mu c_p}{k}$.

Entropy Generation

The following entropy-generation relation is developed to optimize the heat transfer and minimize the energy loss in the system defined in Equations (4)–(6) [3–5, 12, 13].

$$s_{gen} = \frac{k}{\theta_\infty^2}\left(\frac{\partial\theta}{\partial\eta}\right)^2 + \frac{\mu}{\theta_\infty}\left(1+\frac{1}{\beta}\right)\left(\frac{\partial v}{\partial\eta}\right)^2. \quad (7)$$

Using the non-similarity variable, $\partial\theta/\partial\eta = \Delta\theta A^{\frac{1}{3}}v^{-\frac{2}{3}}\partial\theta^*/\partial\eta^*$ and $\partial v/\partial\eta = A^{\frac{2}{3}}v^{-\frac{1}{3}}\partial v^*/\partial\eta^*$ are derived and incorporated into Equation (7), which yields

$$N_s = \left(\frac{\partial\theta}{\partial\eta}\right)^2 + \frac{Br}{\Omega}\left(1+\frac{1}{\beta}\right)\left(\frac{\partial v}{\partial\eta}\right)^2, \quad (8)$$

where

$$N_s = \frac{s_{gen}v^{\frac{4}{3}}\theta^2{}_\infty}{kA^{2/3}(\Delta\theta)^2},\ Br = \frac{\mu A^{\frac{2}{3}}v^{\frac{2}{3}}}{k\Delta\theta},\ \Omega = \frac{\Delta\theta}{\theta_\infty} = \frac{\theta_w-\theta_\infty}{\theta_\infty}.$$

Bejan Number

Bejan is generally considered in the literature to be the first person to point out various factors for optimizing the performance of thermal systems. He developed Bejan's number, which is the ratio of heat-transfer entropy production to total entropy production, and proposed aspects of the second law of thermodynamics that consider various problems

associated with mixed convection. The Bejan number is given by

$$Be = \frac{\frac{k}{\theta_\infty^2}\left(\frac{\partial\theta}{\partial\eta}\right)^2}{\frac{k}{\theta_\infty^2}\left(\frac{\partial\theta}{\partial\eta}\right)^2 + \frac{\mu}{\theta_\infty}\left(1+\frac{1}{\beta}\right)\left(\frac{\partial v}{\partial\eta}\right)^2} \tag{9}$$

and

$$Be = \frac{\left(\frac{\partial\theta}{\partial\eta}\right)^2}{\left(\frac{\partial\theta}{\partial\eta}\right)^2 + \frac{Br}{\Omega}\left(1+\frac{1}{\beta}\right)\left(\frac{\partial v}{\partial\eta}\right)^2}. \tag{10}$$

EXACT SOLUTIONS

In the literature, mixed-convection problems are handled using numerical or approximate methods, and exact solutions are limited. Here, the exact solutions are obtained using the Laplace transform method. Applying the Laplace transform to Equations (4)–(6) gives

$$q\overline{v}(\eta,q) = \left(1+\frac{1}{\beta}\right)\frac{\partial^2\overline{v}(\eta,q)}{\partial\eta^2} + Gr\overline{\theta}(\eta,q) \tag{11}$$

$$\overline{v}(0,q) = \frac{1}{q^2}, \quad \overline{v}(\infty,q) = 0 \tag{12}$$

$$\Pr q\overline{\theta}(\eta,q) = \frac{\partial^2\overline{\theta}(\eta,q)}{\partial\eta^2} \tag{13}$$

$$\overline{\theta}(0,q) = \frac{1}{q}, \quad \overline{\theta}(\infty,q) = 0 \tag{14}$$

The second-order partial differential Equation (13) is solved using the transform boundary conditions (14) as follows.

$$\overline{\theta}(\eta,q) = \frac{e^{-\eta\sqrt{\Pr q}}}{q} \tag{15}$$

Inverting the Laplace transform yields

$$\theta(\eta,\tau) = erfc\left(\frac{\eta\sqrt{\Pr}}{2\sqrt{\tau}}\right) \tag{16}$$

Similarly, the solution of Equation (11) using Equations (12) and (15) is given by

$$\overline{v}(\eta,q) = \frac{a_1}{q^2}e^{-\eta\sqrt{\gamma q}} + \frac{a_0}{q^2}e^{-\eta\sqrt{\Pr q}} \tag{17}$$

where

$$\left(1+\frac{1}{\beta}\right) = \frac{1}{\gamma}, \quad a_0 = \frac{Gr\gamma}{\gamma-\Pr}, \quad a_1 = 1-a_0.$$

With the inverse Laplace transform,

$$v(\eta,\tau) = a_1\left[\left(\frac{1}{2}\eta^2\gamma+\tau\right)erfc\left(\frac{\eta\sqrt{\gamma}}{2\sqrt{\tau}}\right) - \eta\sqrt{\frac{\tau\gamma}{\pi}}e^{\frac{\eta^2\gamma}{4\tau}}\right] + a_0\left[\left(\frac{1}{2}\eta^2\Pr+\tau\right)erfc\left(\frac{\eta\sqrt{\Pr}}{2\sqrt{\tau}}\right) - \eta\sqrt{\frac{\tau\Pr}{\pi}}e^{\frac{\eta^2\Pr}{4\tau}}\right]. \tag{18}$$

Special Case: Note that Equation (18) is reduced to the following form for Newtonian fluid ($\frac{1}{\beta}\to 0$):

$$v(\eta,\tau) = \left(1-\frac{Gr}{1-\Pr}\right)\left[\left(\frac{1}{2}\eta^2+\tau\right)erfc\left(\frac{\eta}{2\sqrt{\tau}}\right) - \eta\sqrt{\frac{\tau}{\pi}}e^{\frac{\eta^2}{4\tau}}\right] + \frac{Gr}{1-\Pr}\left[\left(\frac{1}{2}\eta^2\Pr+\tau\right)erfc\left(\frac{\eta\sqrt{\Pr}}{2\sqrt{\tau}}\right) - \eta\sqrt{\frac{\tau\Pr}{\pi}}e^{\frac{\eta^2\Pr}{4\tau}}\right]. \tag{19}$$

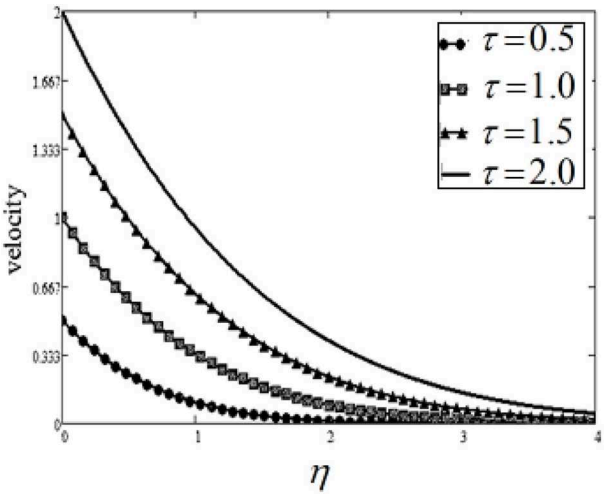

FIGURE 1 | Velocity plot for τ.

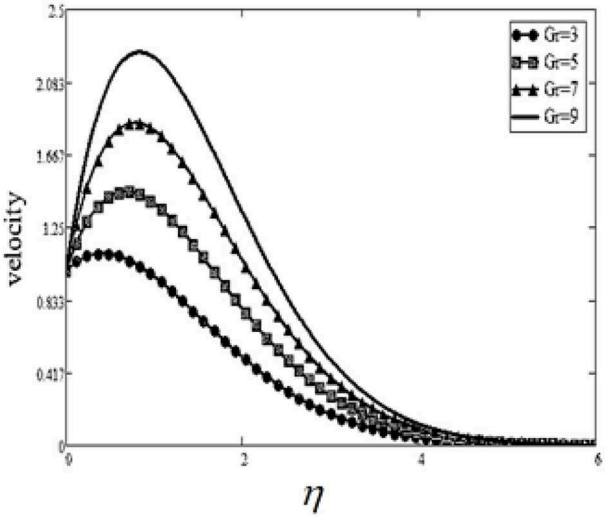

FIGURE 2 | Velocity plot for *Gr*.

Skin Friction

In the dimensionless form, skin friction is defined as

$$c_f = \left(1 + \frac{1}{\beta}\right) \frac{\partial v(\eta, \tau)}{\partial \eta}\bigg|_{\eta=0} \tag{20}$$

Nusselt Number

The heat-transfer rate in the dimensionless form is given by

$$Nu = \frac{\partial \theta(\eta, \tau)}{\partial \eta}\bigg|_{\eta=0} \tag{21}$$

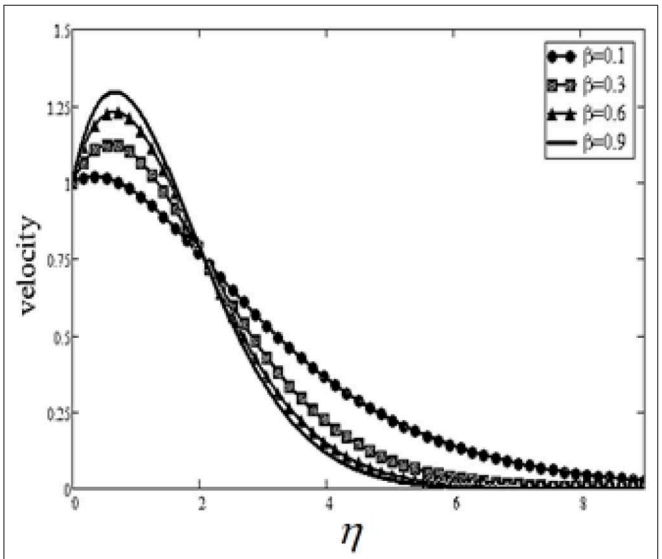

FIGURE 3 | Velocity plot for β.

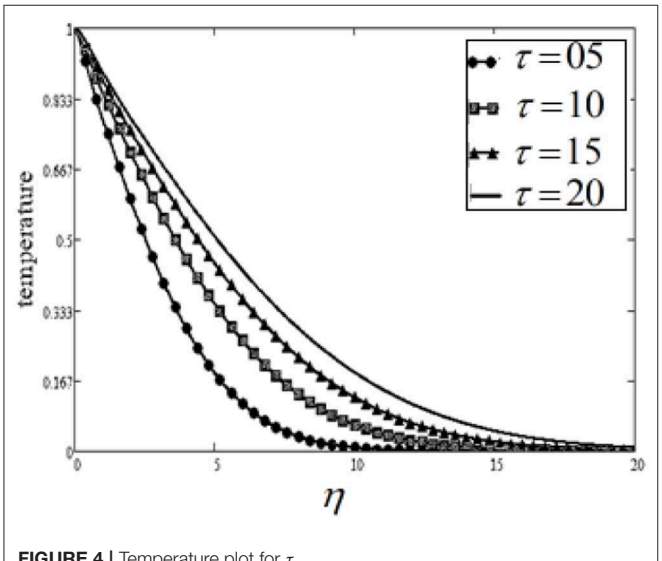

FIGURE 4 | Temperature plot for τ.

RESULTS AND DISCUSSION

In this paper, we conducted an entropy generation (EG) analysis for accelerated flow of non-Newtonian fluid. EG, also known as the second law of thermodynamics, is quite useful in heat transfer problems such as in analyzing heat exchangers. This section highlights the influence of different parameters on velocity, temperature, entropy generation, and Bejan number. Since, in this work, sodium-alginate is taken as a counter-example of a Casson fluid, the Prandtl number (Pr) value is taken as 13.09

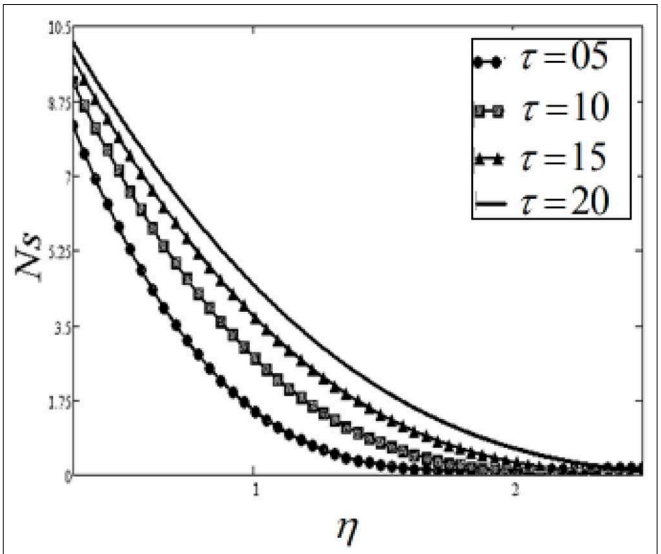

FIGURE 5 | Entropy generation plot for τ.

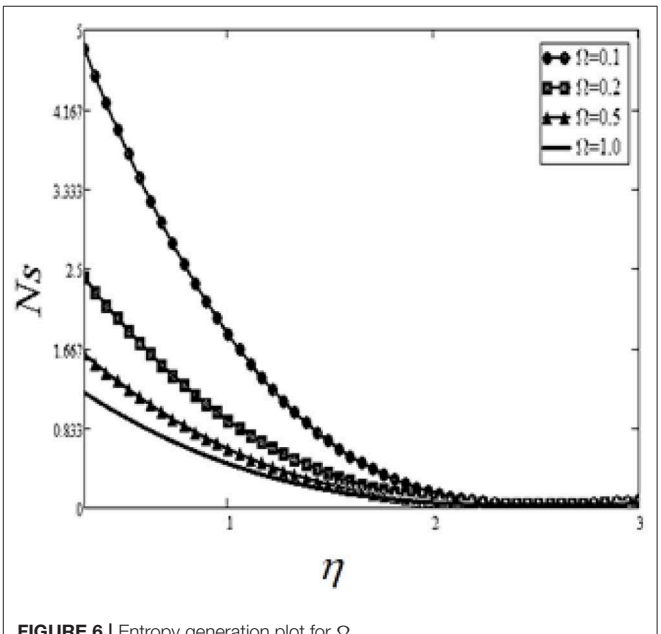

FIGURE 6 | Entropy generation plot for Ω.

in all of these figures. This value of Pr is computed from $\Pr = \mu c_p/k$, $\mu = 0.002$; $k = 0.6376$; $c_p = 4175$.

Figure 1 shows the effects of time τ on velocity. It is found that an increase in time results in an increase in the velocity profile. Physically, the fluid is considered to be unsteady, and thus velocity increases with time. **Figure 2** highlights the effect of *Gr*: the velocity profile increases with increasing *Gr* Value. The increase in *Gr* enhances the buoyancy force, causing the velocity to increase. The physical interpretation indicates that positive values of Gr show heating of the fluid or cooling of the boundary surface. The effect of the Casson parameter, β, is highlighted in **Figure 3**; a dual effect is generated. Initially, near the plate, the velocity is found to increase, and then away from the plate, it decreases for large values of β. This is because an increase in β reduces the boundary-layer thickness. **Figure 4** shows the influence of time τ on the temperature profile, where the maximum values of time τ lead to an increase in temperature.

The impact of EG (*Ns*) for dissimilar values of τ is highlighted in **Figure 5**. An increase in time τ leads to an increase in EG. **Figure 6** presents the EG values for different values of Ω. Ω is defined as the temperature difference, and an increase in temperature difference decreases entropy generation. **Figure 7** presents the influence of unlike values of *Gr* on EG. The buoyancy forces increase with increasing *Gr* values, which results in an

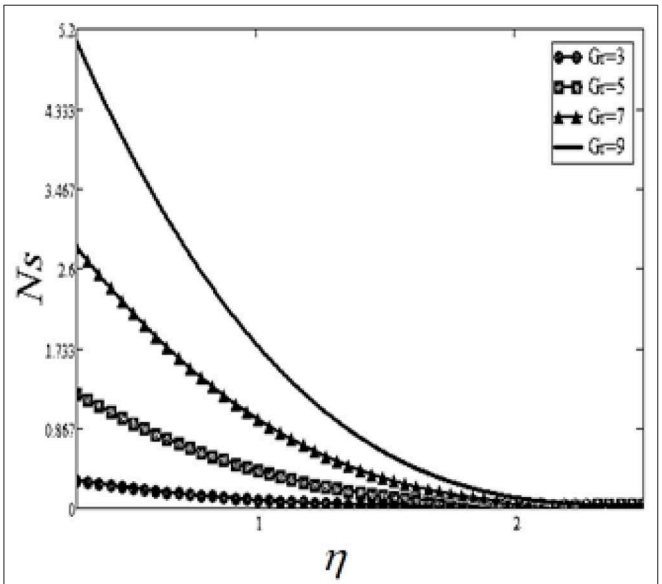

FIGURE 7 | Entropy generation plot for *Gr*.

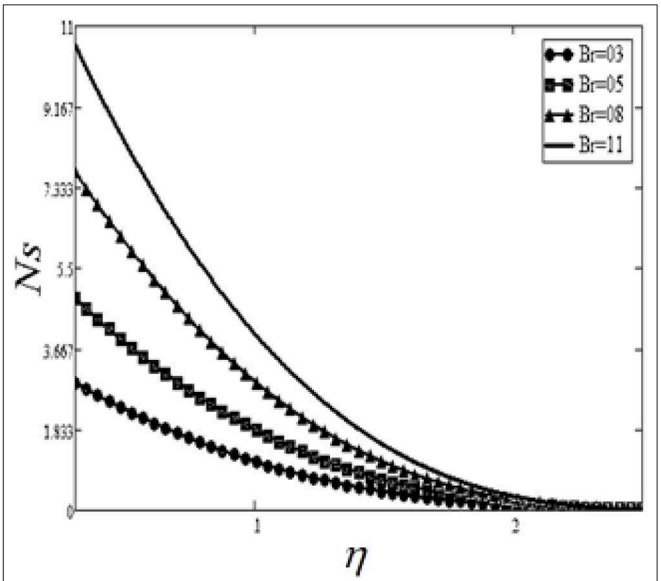

FIGURE 9 | Entropy generation plot for *Br*.

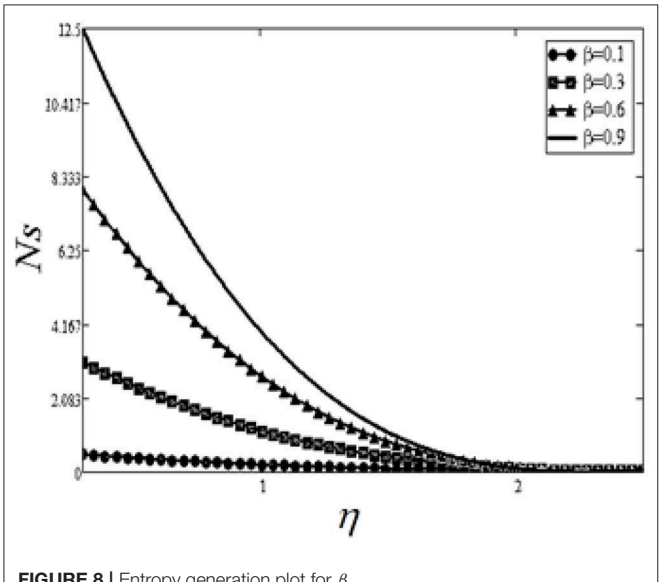

FIGURE 8 | Entropy generation plot for β.

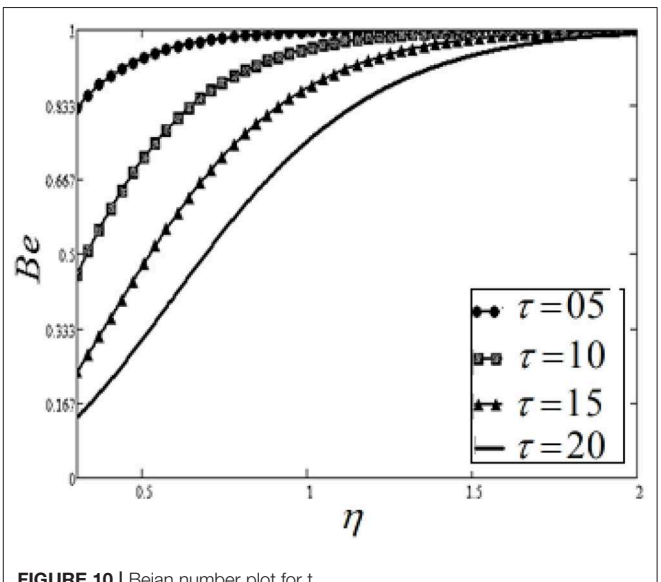

FIGURE 10 | Bejan number plot for t.

increase in entropy generation. In addition, an increase in *Gr* could save energy in the system.

The effect of β is shown in **Figure 8**; it is significant to note that the thickness of the velocity boundary layer decreases with increasing Casson parameter value, and hence EG increases. Furthermore, at high values of β, i.e., $\beta \rightarrow \infty$, Newtonian fluid behavior is observed. The decrease in the Casson parameter leads to an increase in fluid plasticity. The influence of Brickman's number, *Br*, is investigated in **Figure 9**. A large value of Brickman's number produces a high amount of heat via viscous dissipation and vice versa. Therefore, high values of Brickman's number increase entropy generation.

The influence of time parameter τ on Bejan number variation is highlighted in **Figure 10**. The influence of time τ leads to a decrease in Bejan number. **Figure 11** shows the effect of the temperature difference, Ω, on the Bejan number; the maximum value of Ω corresponds with an increase in the Bejan number. **Figure 12** highlights the change in Bejan number with respect to *Gr*. It is detected that a greater *Gr* value decreases the Bejan number. This is because heat-transfer reunification becomes dominant in the region near the plate with increasing *Gr* value. In **Figure 13**, the Bejan number can be seen to decrease with increasing Casson parameter β. The Bejan number variation for different *Br* values is reported in **Figure 14**. Larger values of *Br* are associated with decreasing Bejan number.

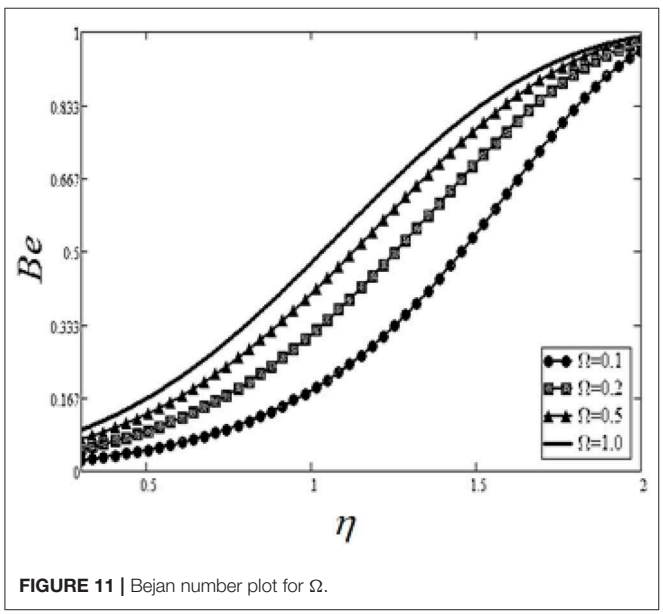

FIGURE 11 | Bejan number plot for Ω.

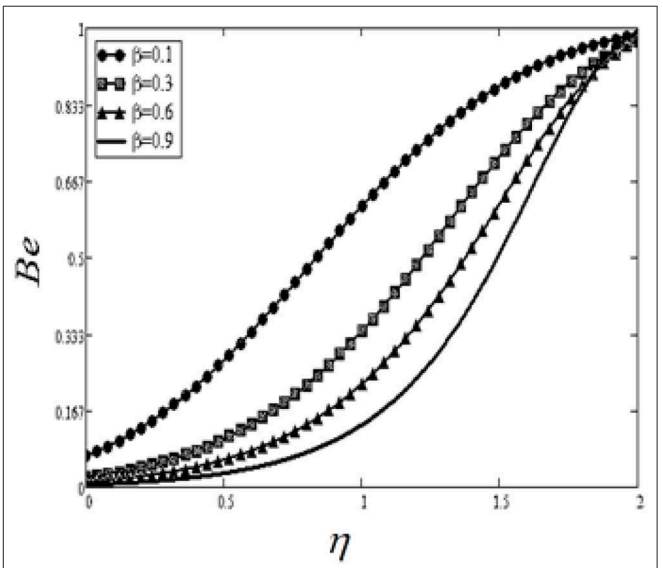

FIGURE 13 | Bejan number plot for β.

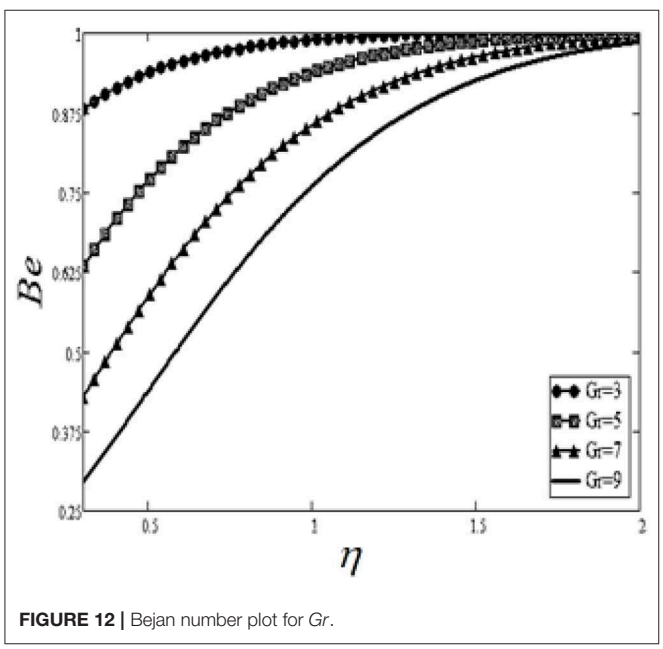

FIGURE 12 | Bejan number plot for *Gr*.

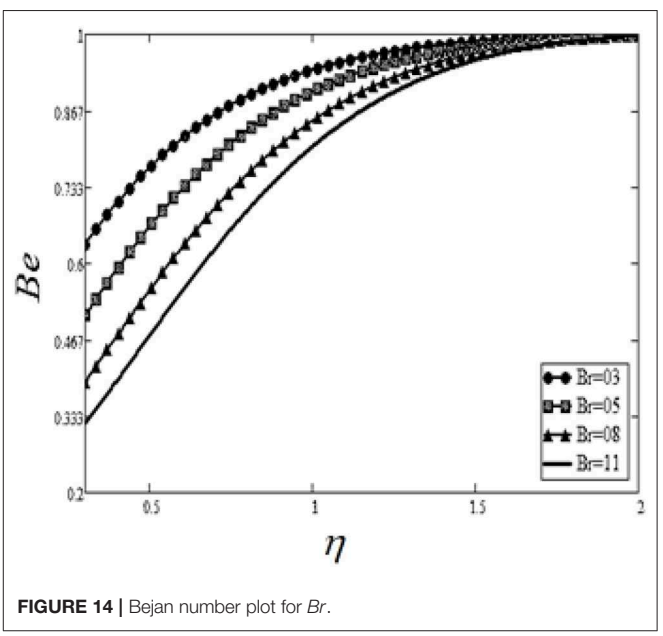

FIGURE 14 | Bejan number plot for *Br*.

TABLE 1 | Effect of variation of different variables on C_f.

t	β	Gr	Pr	C_f
1	0.1	5	0.6	1.5
2				1.811
3				2.05
	0.3			2.147
	0.5			2.219
		7		3.598
		9		5.695
			0.7	1.215
			0.8	0.975

TABLE 2 | Effect of variation of different variables on Nu.

τ	Pr	Nu
1	0.6	0.219
2		0.077
3		0.042
	1.2	0.309
	2.2	0.418

Table 1 examines the effect of different factors on skin friction. It is observed that the skin friction increases with increasing τ, β, and Gr values. **Table 2** highlights the effect of the variation in τ and Pr on Nusselt number. The Nusselt number decreases up to the maximum value of τ and increases for the maximum value of Pr.

CONCLUDING REMARKS

An exact analysis of entropy generation in sodium-alginate fluid over an accelerated heated plate is conducted via Laplace-transform methods. The Bejan number Be and local entropy generation Ns are discussed for various parameters. The effects are displayed for different embedded parameters. The main conclusions are:

- For maximum entropy generation Ns, we need to maximize the t, Gr, β, and Br values. In contrast, for minimum values, we need to minimize the Pr and Ω values.
- For the maximum Bejan number, Be, we need to maximize the Pr and Ω values. In contrast, for minimum values, we need to minimize the t, Gr, β, and Br values.
- The Casson parameter, β, exhibits dual effects.

AUTHOR CONTRIBUTIONS

TA formulated and solved the problem. IK plotted and discussed the results and revised the manuscript. TA and IK wrote the manuscript.

ACKNOWLEDGMENTS

The authors acknowledge with thanks the Deanship of Scientific Research (DSR) at Majmaah University, Majmaah, Saudi Arabia, for technical and financial support through vote number 38/107 for this research project.

REFERENCES

1. Mahian O, Kianifar A, Sahin AZ, Wongwises S. Entropy generation during Al2O3/water nanofluid flow in a solar collector: effects of tube roughness, nanoparticle size, and different thermophysical models. *Int J Heat Mass Transf.* (2014) **78**:64–75. doi: 10.1016/j.ijheatmasstransfer.2014.06.051
2. Mahian O, Mahmud S, Heris SZ. Effect of uncertainties in physical properties on entropy generation between two rotating cylinders with nanofluids. *J Heat Transf.* (2012) **134**:101704. doi: 10.1115/1.4006662
3. Bejan A. Second-law analysis in heat transfer and thermal design. *Adv Heat Transf.* (1982) **15**:1–58. doi: 10.1016/S0065-2717(08)70172-2
4. Bejan A. *Entropy Generation Minimization: The Method of Thermodynamic Optimization of Finite-Size Systems and Finite-Time Processes*. Boca Raton: CRC Press (1995).
5. Bejan A. A study of entropy generation in fundamental convective heat transfer. *ASME J Heat Transf.* (1979) **101**:718–25. doi: 10.1115/1.3451063
6. Selimefendigil F, Öztop HF, Abu-Hamdeh N. Natural convection and entropy generation in nanofluid filled entrapped trapezoidal cavities under the influence of magnetic field. *Entropy.* (2016) **18**:43. doi: 10.3390/e18020043
7. Qing J, Bhatti MM, Abbas MA, Rashidi MM, Ali MES. *Entropy* generation on MHD Casson nanofluid flow over a porous stretching/shrinking surface. *Entropy.* (2016) **18**:123. doi: 10.3390/e18040123
8. Mahian O, Kianifar A, Kleinstreuer C, Moh'd AAN, Pop I, Sahin AZ, et al. A review of entropy generation in nanofluid flow. *Int J Heat Mass Transf.* (2013) **65**:514–32. doi: 10.1016/j.ijheatmasstransfer.2013.06.010
9. Darbari B, Rashidi S, Abolfazli Esfahani J. Sensitivity analysis of entropy generation in nanofluid flowinside a channel by response surface methodology. *Entropy.* (2016) **18**:52. doi: 10.3390/e18020052
10. Ellahi R, Hassan M, Zeeshan A. Shape effects of nanosize particles in Cu–H2O nanofluid on entropy generation. *Int J Heat Mass Transf.* (2015) **81**:449–56. doi: 10.1016/j.ijheatmasstransfer.2014.10.041
11. Sheikholeslami M, Ashorynejad HR, Rana P. Lattice Boltzmann simulation of nanofluid heat transfer enhancement and entropy generation. *J Mol Liquids.* (2016) **214**:86–95. doi: 10.1016/j.molliq.2015.11.052
12. Saqib M, Ali F, Khan I, Sheikh NA, Khan A. Entropy generation in different types of fractionalized nanofluids. *Arab J Sci Eng.* (2019) **44**:531–40. doi: 10.1007/s13369-018-3342-8
13. Khan A, Khan I, Alkanhal TA, Ali F, Khan D, Nisar KS. Entropy generation in MHD conjugate flow with wall shear stress over an infinite plate: exact analysis. *Entropy.* (2019) **21**:359. doi: 10.3390/e21040359
14. Bhatti M, Abbas T, Rashidi M, Ali M, Yang Z. Entropy generation on MHD Eyring–Powell nanofluid through a permeable stretching surface. *Entropy.* (2016) **18**:224. doi: 10.3390/e18060224
15. Li Z, Sheikholeslami M, Jafaryar M, Shafee A, Chamkha AJ. Investigation of nanofluid entropy generation in a heat exchanger with helical twisted tapes. *J Mol Liquids.* (2018) **266**:797–805. doi: 10.1016/j.molliq.2018.07.009
16. Khan A, Khan D, Khan I, Ali F, ul Karim F, Imran M. MHD flow of Sodium Alginate-based Casson type nanofluid passing through a porous medium with Newtonian heating. *Sci Rep.* (2018) **8**:8645. doi: 10.1038/s41598-018-26994-1
17. Haq SU, Khan I, Ali F, Abdelhameed TN. Influence of slip condition on unsteady free convection flow of viscous fluid with ramped wall temperature. *Abst Appl Anal.* (2015) **2015**:327975. doi: 10.1155/2015/327975
18. Khan I, Abdelhameed TN, Dennis LC. Heat transfer in eccentric-concentric rotation of a disk and fluid at infinity. *J Comp Theor Nanosci.* (2016) **13**:6482–7. doi: 10.1166/jctn.2016.5590

19. Ahmed TN, Khan I. Mixed convection flow of sodium alginate (SA-NaAlg) based molybdenum disulphide (MoS2) nanofluids: Maxwell Garnetts and Brinkman models. *Results Phys.* (2018) **8**:752–7. doi: 10.1016/j.rinp.2018.01.004
20. Khater AH, Callebaut DK, Abdul-Aziz SF, Abdelhameed TN. Potential symmetry and invariant solutions of Fokker–Planck equation modelling magnetic field diffusion in magnetohydrodynamics including the Hall current. *Phys A*. (2004) **341**:107–22. doi: 10.1016/j.physa.2004.04.118
21. Khater AH, Callebaut DK, Abdelhameed TN. Potential symmetry and invariant solutions of Fokker-Planck equation in cylindrical coordinates related to magnetic field diffusion in magnetohydrodynamics including the Hall current. *Eur Phys J B Condens Matter Complex Syst.* (2006) **50**:17. doi: 10.1140/epjb/e2006-00138-5

Conflict of Interest: The authors declare that the research was conducted in the absence of any commercial or financial relationships that could be construed as a potential conflict of interest.

NOMENCLATURE

u -Velocity of the fluid, $[ms^{-1}]$
θ -Temperature of the fluid, $[K]$
g -Acceleration due to gravity, $[ms^{-2}]$
c_p -Specific heat at a constant pressure, $[jkg^{-1}K^{-1}]$
Gr -Thermal Grasshof number, $(= \beta T_w)$
k -Thermal conductivity of the fluid, $[Wm^{-2}K^{-1}]$
Nu -Nusselt number, [–]
Pr -Prandtl number, $(= \mu c_p/k)$
θ_∞ -Fluid temperature far away from the plate, $[K]$
q -Laplace transforms parameter
A -Arbitrary constant $[ms^{-2}]$

GREEK SYMBOLS

ν -Kinematic viscosity of the fluid, $[m^2s^{-1}]$
μ -Dynamic viscosity, $[kgm^{-1}s^{-1}]$
ρ -Fluid density, $[kgms^{-3}]$
β_θ -Volumetric coefficient of thermal expansion,$[K^{-1}]$
β -Casson fluid parameter
B_γ-Brinkman number
Ω -Dimensionless temperature function